Available online at www.sciencedirect.com
SCIENCE DIRECT®
Journal of Luminescence 119–120 (2006) 228–232
JOURNAL OF LUMINESCENCE
www.elsevier.com/locate/jlumin

Excitonic properties of vertically aligned ZnO nanotubes under high-density excitation

Y.M. Lu*, H.W. Liang, D.Z. Shen, Z.Z. Zhang, J.Y. Zhang, D.X. Zhao, Y.C. Liu, X.W. Fan

Laboratory of Excited State Processes, Chang Chun Institute of Optics, Fine Mechanics and Physics, Chinese Academy of Sciences, 16-Dongnahu Road, 130033 Changchun, PR China

Available online 2 February 2006

Abstract

In this paper, highly oriented and vertically arranged ZnO nanotubes are prepared on Al_2O_3 (0 0 0 1) substrate without employing any metal catalysts by plasma-assisted molecular beam epitaxy. The photoluminescence (PL) spectra at room temperature are studied under high excitation densities. Under lower excitation density ($<60\,kW/cm^2$), PL spectrum shows that one strong free exciton emission (FE) locates at 3.306 eV. As the excitation density increases up to $200\,kW/cm^2$, a new emission peak (P_n) located at low-energy side of FE is attributed to the spontaneous emission due to an exciton–exciton (E_x–E_x) scattering process from two ground state excitons, where one exciton is recombined by emitting a photon and the other is scattered into the excited states of $n = 2, 3, 4 \ldots \infty$. Under excitation density of $300\,kW/cm^2$, the stimulated emission originating from E_x–E_x scattering is obtained. When the excitation density is above $580\,kW/cm^2$, the emission from electron–hole plasma is observed in low-energy side of the P band and indicates a typical superradiation recombination processes with increasing excitation density.

PACS: 81.07.D; 71.35; 78.45; 52.27.E; 42.50.F

Keywords: ZnO nanotube; Exciton–exciton scattering; Stimulated emission; Electron–hole plasma; Superradiation process

1. Introduction

ZnO has a band gap of 3.37 eV at room temperature (RT) and extremely large exciton binding energy of 59 meV [1], which in principle allows the exciton governed luminescence at short wavelengths to be dominant at RT. In particular, the corresponding enhancement of exciton gain in low-dimension structure makes it possible to apply RT strong exciton effects to realize ultraviolet (UV) laser devices. Therefore, the study on the origin of stimulated emission and the mechanism

*Corresponding author. Tel.: +86 431 5682964; fax: +86 431 5682964.
E-mail address: ymlu@mail.jl.cn (Y.M. Lu).

0022-2313/$ - see front matter © 2006 Elsevier B.V. All rights reserved.
doi:10.1016/j.jlumin.2005.12.035

of optical gain has attracted much attention [2–4]. RT-stimulated emission and optically pumped laser action from ZnO thin films and its quantum well structure have been reported [5,6]. These reported stimulated emissions were originated from an exciton–exciton (E_x–E_x) scattering or an electron–hole plasma (EHP) under different excitation conditions [7].

One-dimensional semiconductors have become the important fundamental building blocks because of their fundamental physical properties and their potential applications for nanoelectronic and nanophotonic devices [8,9]. Recent progress in stimulated emission has been achieved from a variety of low-dimensional ZnO structures such as nanowires [10–12], nanorods [13,14] and nanoribbons [15]. To understand which of EHP processes and exciton recombination is more efficient radiative process in such nanostructure, the investigation of excitonic properties is essential under different excitation conditions.

In this letter, we report excitonic properties of vertically arranged ZnO nanotubes under different excitation densities. A stimulated emission due to E_x–E_x scattering in medium excitation density was observed at RT. Under higher excitation density, a superradiation emission caused by EHP process was obtained.

2. Experiment

A V80 H molecular-beam epitaxy (MBE) system was employed for growing the ZnO nanotubes, where Knudsen effusion cells were used to evaporate elemental zinc with 99.9999% purity. Atomic oxygen was generated from ultra-pure O_2 gas (99.999%) activated by an Rf atomic source with an electrostatic ion trap operating at 500 V during growth. Al_2O_3 substrates with a well-polished (0 0 0 1) face were pretreated at 800 °C in ultrahigh vacuum ($<1\times10^{-8}$ mbar) for 30 min to remove the surface contaminants. Prior to growth, the chemical-treated substrate was exposed in O-plasma at 550 °C for 40 min. Firstly, a very thin ZnO layer (about 3 nm) was grown and then treated by O-plasma for 30 min. Sequentially, ZnO was deposited on this buffer for 2 h in same condition. In the growth process, Zn steam and O_2 partial pressure in the growth chamber were fixed at 4×10^{-4} and 6×10^{-3} Pa, respectively.

After growth, the sample morphology was confirmed by filed emission scanning electron microscope (FE-SEM) and high-resolution transmission electron microscope (TEM). Photoluminescence (PL) spectra were measured at RT. A He–Cd laser with the 325 nm (50 mw) line was used as the excitation source and a JY63 Raman spectrometer was employed to detect the luminescence signals. Optical pumping experiments were performed using the 320 nm lines of a mode-locked Ti:sapphire laser. The laser output was generated by an optical parametric amplifier (OPA) providing pulses with duration of 200 fs at a frequency of 1 kHz. The excitation light was focused on the sample surface using a cylindrical lens. Emission from the sample edge was collected into a spectrometer and was detected by an electrically cooled charge-coupled device (CCD).

3. Results and discussion

The FE-SEM images of the surface morphology of the samples are shown in Fig. 1(a). The nanotubes with surface density of $7\times10^{8}\,cm^{-2}$ have a regular alignment which is perpendicular to the *c*-plane of Al_2O_3 substrate. The inset of

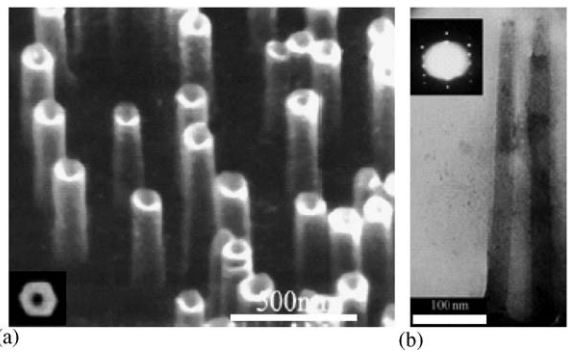

Fig. 1. ZnO nanotubes grown on Al_2O_3 substrates. (a) FE–SEM image tilted 45° view, the inset gives a top view of one nanotube. (b) High-resolution TEM image of one nanotube side view.

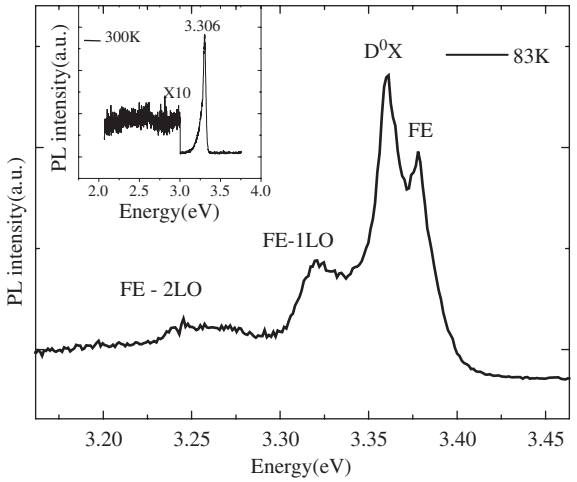

Fig. 2. The PL spectra of ZnO nanotubes at 83 K and RT (inset) excited by the 325 nm line of a He–Cd laser.

Fig. 1(a) shows the top view SEM image of one nanotube. It can be seen clearly that much regular hexagonal ZnO nanotube with wurtzite structure was formed. A high-resolution TEM image indicates that the nanotube has a uniform diameter of 120 nm, a height of 500 nm and a wall thickness about 25 nm, as shown in Fig. 1(b).

Fig. 2 shows PL spectra at 83 K and RT excited by a He–Cd laser with 325 nm line. At RT, as seen in the inset of Fig. 2, one UV peak with a narrow width of 41.5 meV is located at 3.303 eV. It should be noted that this energy value is higher than of free exciton in bulk ZnO [16]. In order to study the origin of UV emission, a PL measurement at various temperatures was performed. Fig. 2 shows the PL spectra measured at 83 K. Four evident emission peaks labeled FE, D^0X, FE-LO and FE-2LO can be observed, respectively. As reported in Ref. [18], the FE and D^0X peaks located at 3.377 and 3.359 eV were attributed to the emission of free exciton and the recombination of excitons bound to neutral donors, respectively. For FE, FE-LO and FE-2LO bands, we note that these peaks have equal energy spacing of about 70 meV, which is in good agreement with the energy of the LO phonons of ZnO [16]. This implies that FE-LO and FE-2LO bands are the corresponding first and second LO phonon peaks of the FE, respectively. By measuring PL spectra at different temperatures (not shown here), we found that the emission of bound-exciton rapidly decreases with increasing temperatures so that the emission of free exciton dominantly contributes to the PL spectrum at RT, as shown in the inset of Fig. 2.

At RT optical pumping experiment of the nanotubes are studied under high excitation density using a pulsed Ti:sapphire laser. Figs. 3(a) and (b) exhibit the measured PL spectra under different excitation densities. When excitation density is less than 60 kW/cm^2, one UV emission located at 3.302 eV is observed. As a comparison, the PL spectrum excited using the 325 nm line of a He–Cd laser is also shown in the bottom trace of Fig. 3 (a). It is clearly seen that this UV peak of 3.302 eV is originating from the free exciton emission (FE). As the excitation density increases to 200 kW/cm^2, a new emission peak (P_2) is observed in 82 meV below the FE band. We considered that P_2 band is from the spontaneous emission due to an E_x–E_x scattering process, where one exciton recombine by emitting a photon and the other one is scattered into the excited state of $n = 2$. This is consistent with the reported result in ZnO thin films by Bagnall et al. [2]. For the process of E_x–E_x scattering, the photon energies were given by [17]

$$E_n = E_{ex} - (1 - 1/n^2)E_{ex}^B - 3kT/2 \quad (n = 2, 3, 4, \ldots), \tag{1}$$

where E_n is the emitted photon energy, E_{ex} is the exciton emission energy, E_{ex}^B is the binding energy of the free exciton, n is the quantum number, and kT is the thermal energy. At RT, $3kT/2$ is about 38.7 meV.P_2 band energy of 3.220 eV is given by the PL spectrum. The calculated value of E_{ex}^B using formula (1) is 58 meV, which is very close to the value of the exciton-binding energy in ZnO bulk crystal (59 meV) [1]. This means that P_2 band is due to the recombination process of E_x–E_x scattering in which one of the excitons is scattered into $n = 2$ state. With increasing the excitation density up to 260 kW/cm^2, another new peak (P band) appears at the low-energy shoulder of the P_2 band. The full-width at half-maximum (FWHM)

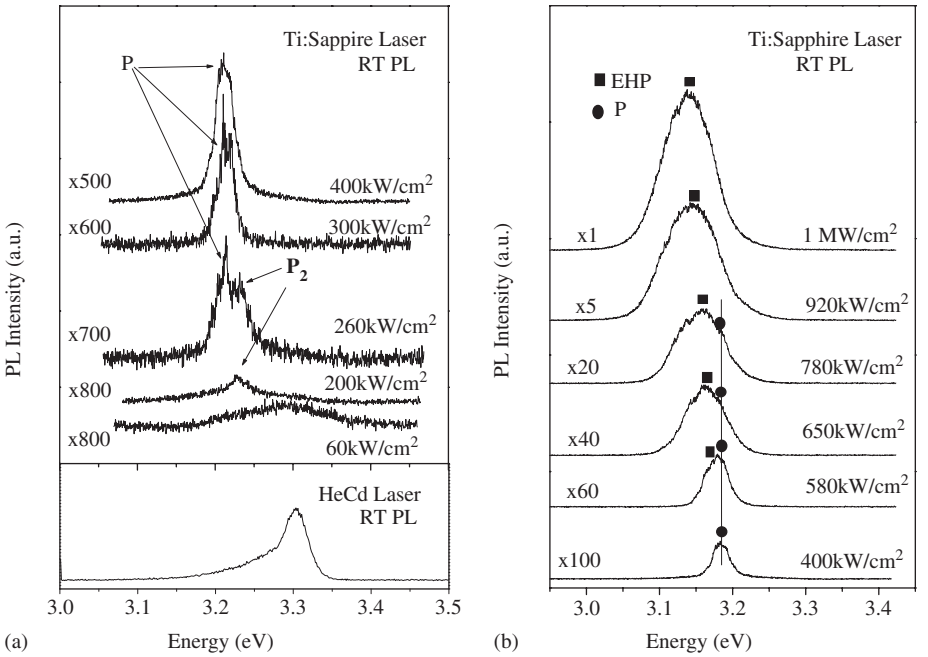

Fig. 3. RT PL spectra under various excitation densities. (a) The upper curves show spontaneous and stimulated emission spectra with increasing the excitation intensity from 60 to 400 kW/cm^2 provided by using a mode-locked Ti:sapphire laser. The lower curve shows PL spectrum excited by the 325 nm line of a HeCd laser. (b) PL spectra under higher excitation intensities varying from 400 kW/cm^2 to 1 MW/cm^2 provided by using a mode-locked Ti:sapphire laser.

of this P band is narrower than that of P_2 band. We attributed P band to be from the radiative recombination due to E_x–E_x scattering process with one exciton scattered into the higher exciton state near continuum states. Note that the PL integrated intensity of P band increases superlinearly and FWHM becomes rather narrow when the excitation density is up to 300 kW/cm^2. The superlinear increase of the emission intensity and the sharpening of the emission peak with increasing excitation density above a threshold indicate the typical nature of a stimulated emission. When the excitation density exceeds 580 kW/cm^2, a new band (■) appears in low-energy side of P band. The position of this peak shifts to low energy and the line width broadens with increasing the excitation density. In this case, the increase of P band intensity is restrained and there is no peak shift (●) with increasing excitation density, as shown in Fig. 3(b). Under high excitation density, the redshift and broadening of emission peak is a sign of emergence of EHP, in which high-density carriers result in the effects of the exciton screening and the band-gap renormalization.

The integrated emission intensity (I) versus excitation density (I_{ex}) is plotted in Fig. 4. From Fig. 4, we found that the intensity of the FE band grows linearly with I_{ex} while the intensity of P_2 band increase in proportion to the square of I_{ex}, which is consistent with the fact that they are the free excitonic emission and a spontaneous emission due to E_x–E_x scattering, respectively. At I_{ex} above a threshold, the intensity of P band rapidly increases following the relation of I_{ex}^4, clearly demonstrating the stimulated emission caused by optical gain due to E_x–E_x scattering. Further increasing I_{ex}, the intensity of EHP band gives also superlinear growth, $I \propto I_{ex}^4$, indicating a typical property of the superradiation recombination. This fact supports further that the EHP process has the larger optical gain and may cause stimulated emission.

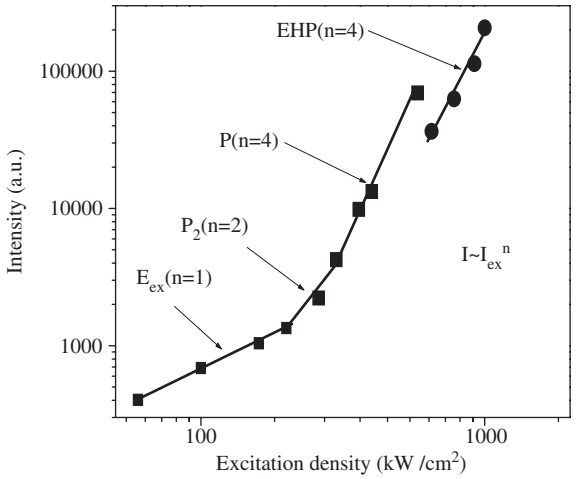

Fig. 4. The integrated intensities (I) of PL emission bands as a function of the excitation densities (I_{ex}).

4. Conclusions

In summary, we have performed a detailed study about RT excitonic properties of ZnO nanotubes under high excitation density. At the excitation density below 60 kW/cm^2, PL spectrum shows a FE located at 3.377 eV. As the excitation density increase up to 200 kW/cm^2, P band due to E_x–E_x scattering is observed in low-energy side of the FE and the intensity grows superlinearly with increasing excitation density. When the excitation density is above 200 kW/cm^2, the stimulated emission originating from E_x–E_x scattering is obtained. Further increasing excitation density, the emission from EHP appears in low-energy side of the P band, and indicates a typical super-radiation recombination processes with increasing excitation density.

Acknowledgments

This work is supported by the "863" High Technology Research Program in China, under Grant no 2001AA311120, the Key Project of National Natural Science Foundation of China under Grant no 60336020, the Innovation Project of Chinese Academy of Sciences, the National Natural Science Foundation of China under Grant no 60278031, no 60376009, and no 50402016.

References

[1] Y.F. Chen, H.J. Ko, S.K. Hong, T. Yao, Appl. Phys. Lett. 76 (2000) 559.
[2] Z.K. Tang, G.K.L. Wong, P. Yu, M. Kawasaki, A. Ohtomo, H. Koinuma, Y. Segawa, Appl. Phys. Lett. 72 (1998) 3270.
[3] Ü. Özgür, A. Teke, C. Liu, S.J. Cho, H. Morkoc, H.O. Everitt, Appl. Phys. Lett. 84 (2004) 3223.
[4] A.N. Gruzintsev, V.T. Volkov, C. Barthou, P. Benalloul, J.M. Frigerio, Thin Solid Films 459 (2004) 262.
[5] D.M. Bagnall, Y.F. Chen, Z. Zhu, T. Yao, S. Koyama, M.Y. Shen, T. Goto, Appl. Phys. Lett. 70 (1997) 2230.
[6] H.D. Sun, T. Makino, N.T. Tuan, Y. Segawa, M. Kawasaki, A. Ohtomo, K. Tamura, H. Koinuma, Appl. Phys. Lett. 78 (2001) 2464.
[7] P. Yu, Z.K. Tang, G.K.L. Wong, M. Kawasaki, A. Ohtomo, H. Koinuma, Y. Segawa, Solid State Commun. 103 (1997) 459.
[8] X.F. Duan, Y. Huang, R. Agarwal, C.M. Lieber, Nature 421 (2003) 241.
[9] S.S. Wong, E. Joselevich, A.T. Woolley, C.L. Cheung, C.M. Lieber, Nature 394 (1998) 52.
[10] J.H. Choy, E.S. Jang, J.H. Won, J.H. Chung, D.J. Jang, Y.W. Kim, Appl. Phys. Lett. 84 (2004) 287.
[11] J.C. Johnson, H.Q. Yan, P.D. Yang, R.J. Saykally, J. Phys. Chem. B 107 (2003) 8816.
[12] Z.R. Qiu, K.S. Wong, M.M. Wu, W.J. Lin, H.F. Xu, Appl. Phys. Lett. 84 (2004) 2739.
[13] J.H. Choy, E.S. Jang, J.H. Won, J.H. Chung, D.J. Jang, Y.W. Kim, Adv. Mater. 15 (2003) 1911.
[14] A.B. Hartanto, X. Ning, Y. Nakata, T. Okada, Appl. Phys. A 78 (2004) 299.
[15] H.Q. Yan, J. Johnson, M. Law, R.R. He, K. Knutsen, J.R. McKinney, J. Pham, R. Saykally, P.D. Yang, Adv. Mater. 15 (2003) 1907.
[16] D.W. Hamby, D.A. Lucca, M.J. Klopfstein, G. Cantwell, J. Appl. Phys. 93 (2003) 3214.
[17] C. Klingshirn, Phys. Status Solidi B 71 (2) (1975) 547.
[18] L.J. Wang, N.C. Giles, J. Appl. Phys. 94 (2003) 973.